CHAPTER III
EXPERIMENTAL

3.1 The Experimental Loop

The model developed is used to predict the corrosion rate of 95 feeder pipes of the nuclear reactor at Point Lepreau Nuclear Generating Station. The diagram of feeders is shown in Figure 3.1. This model is also used to predict corrosion rate of the probes in the test loop as illustrated in Figure 3.2.

The purpose of this test experimental loop, is to study flow-assisted corrosion so it is called the FAC loop. The FAC loop simulates the primary coolant loop of a CANDU reactor, so the conditions in the experimental loop and in the CANDU reactor at the plant are as similar as possible. Temperature is 265°C and 310°C for inlet and outlet feeders, respectively.

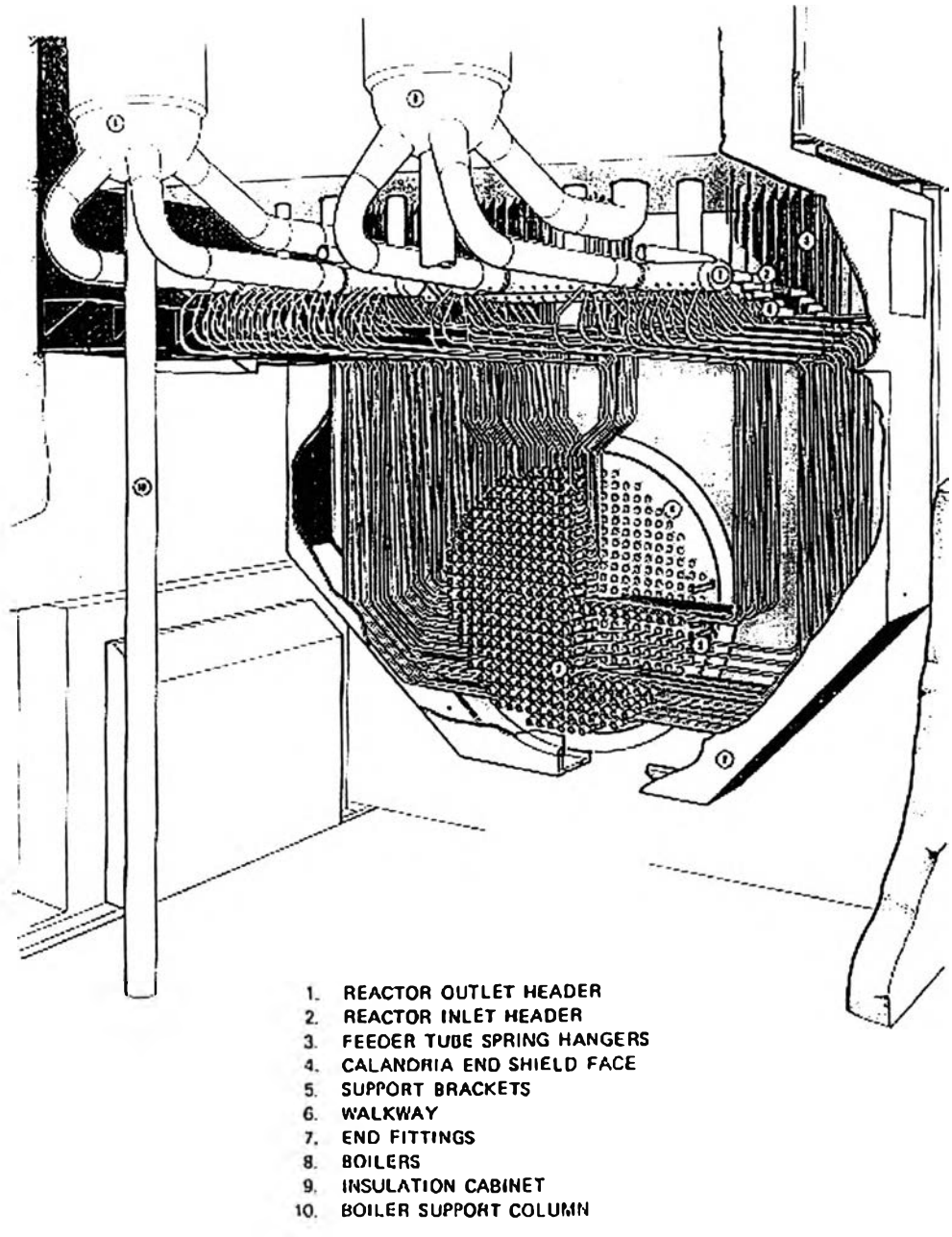

Figure 3.1 Diagram of feeders in the CANDU reactor.

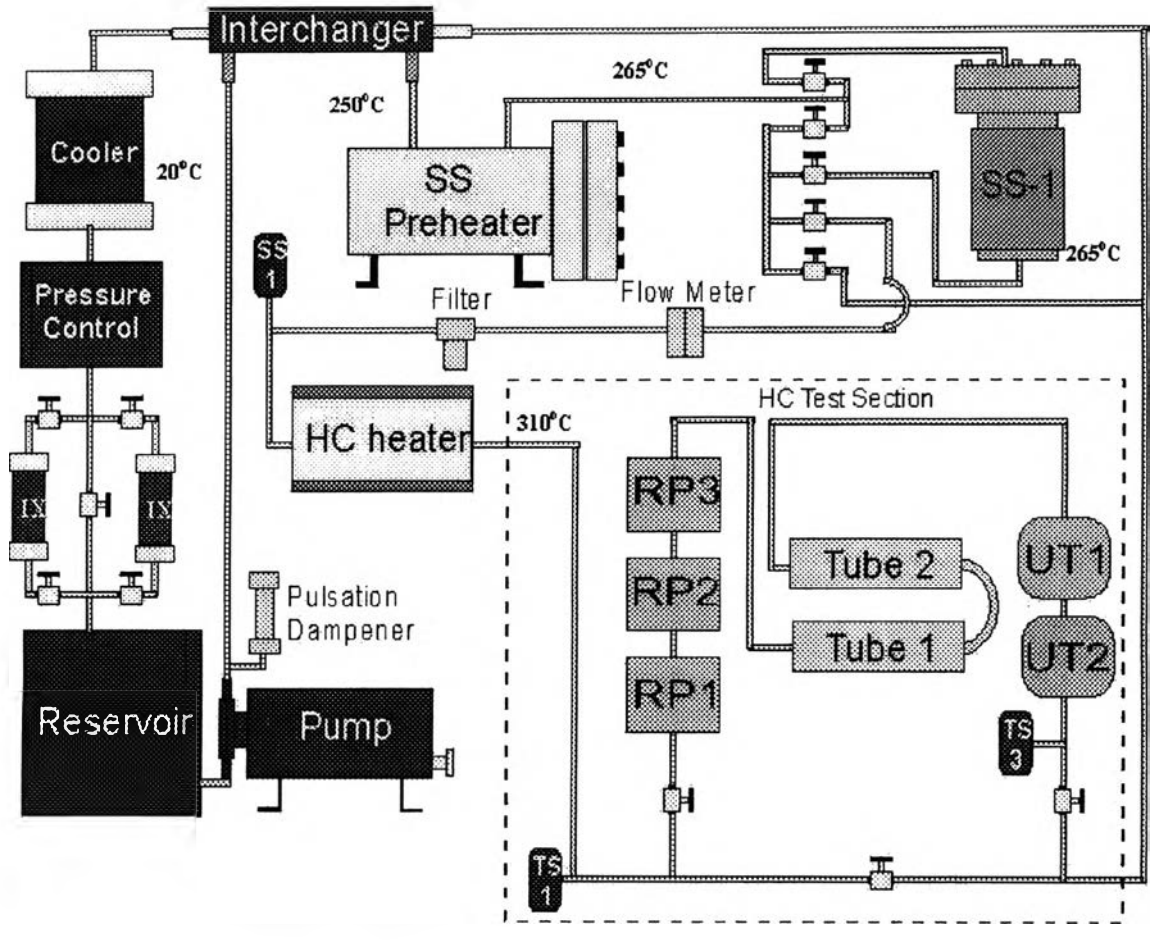

Figure 3.2 Experimental loop.

The coolant is pumped from the reservoir to the heater and the temperature increases to 265°C (the same temperature as at the inlet feeders). The coolant flows to the SS unit which saturates the coolant in dissolved iron. The HC heater is an inert unit and acts as the reactor core in the plant, so the coolant temperature is 310°C after passing this unit. The coolant which has the same conditions as the coolant in outlet feeders flows from HC heater unit to the test loop. In the test loop, there are three kinds of probe that represent outlet feeder pipes in the CANDU reactor: 1) tube probes, 2) wire resistance probes and 3) ultrasonic probes. All probes are A106-B stainless steel, the same material as feeders in CANDU reactor.

1) The tube probe has a geometry close to the feeder pipes. Therefore,

the tube probe is better than for demonstrations geometric effects. The metal loss can be obtained by measuring the electrical resistance of the probe and a calculation by Eq.3.1.

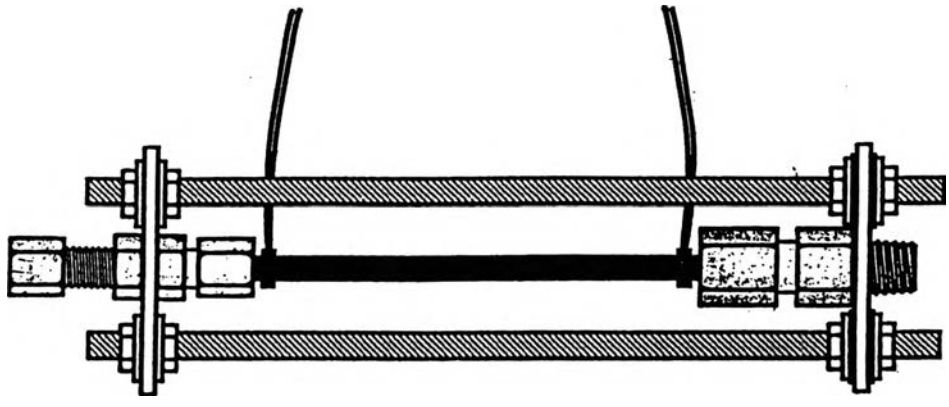

Figure 3.3 The tube probe in the test loop.

$$R = \frac{\rho \times l}{A} \tag{3.1}$$

where R = electric resistance

ρ = resistivity of the probe

l = the length for tube probe

A = cross sectional area.

For tube probe,

$$A = \pi(r_o^2 - r_i^2) \tag{3.2}$$

where r_o = outside diameter

r_i = inside diameter.

From Eq.3.1, the resistance is inversely proportional to the cross sectional area or the tube. Electrical resistance can be directly related to metal loss.

2)The wire resistance probe is a carbon steel wire fixed inside a zirconia tube giving an annulus. To evaluate metal loss, the same method as for the tube probes is used and metal loss can be directly related to change in resistance.

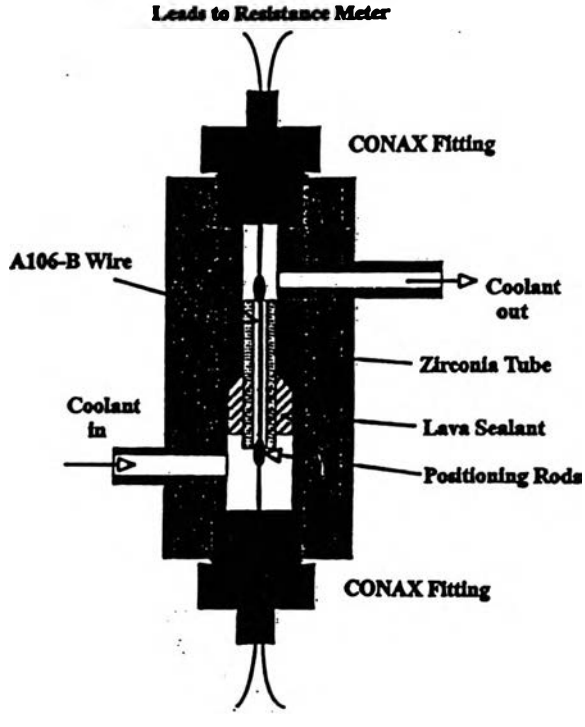

Figure 3.4 The wire probe in the test loop.

3) The ultrasonic probe in the FAC loop is shown in Figure 3.5. The coolant flows in the titanium tube, and passes a jet orifice which strikes the A106-B carbon steel coupon. The thickness change of the coupon is measured by a device called a transducer. This technique is also used as an on-line device to measure the thickness of feeders of the CANDU reactors in the plant.

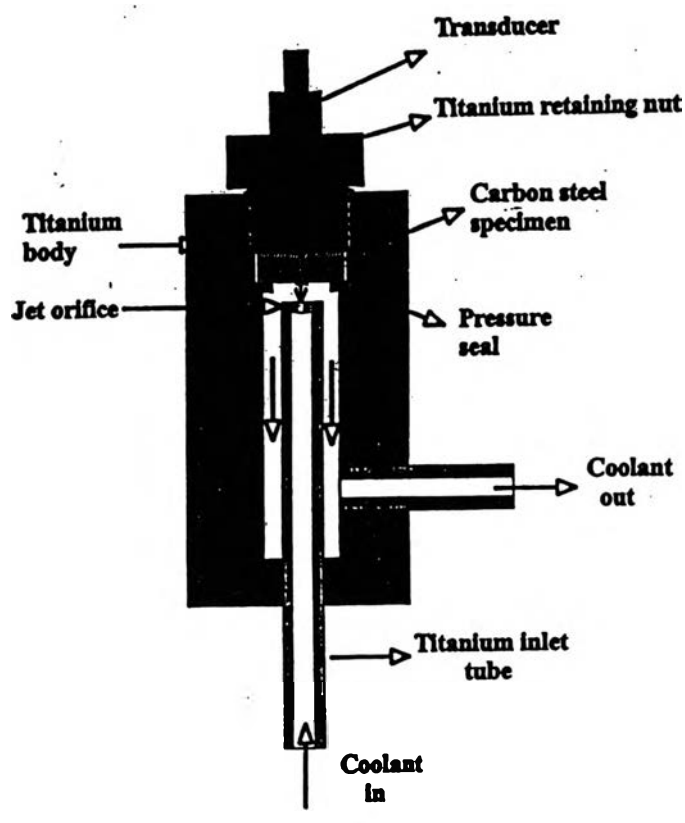

Figure 3.5 The ultrasonic probe in the test loop.

3.2 Model and Mechanisms

In this model, there are many mechanisms affecting feeder thinning.

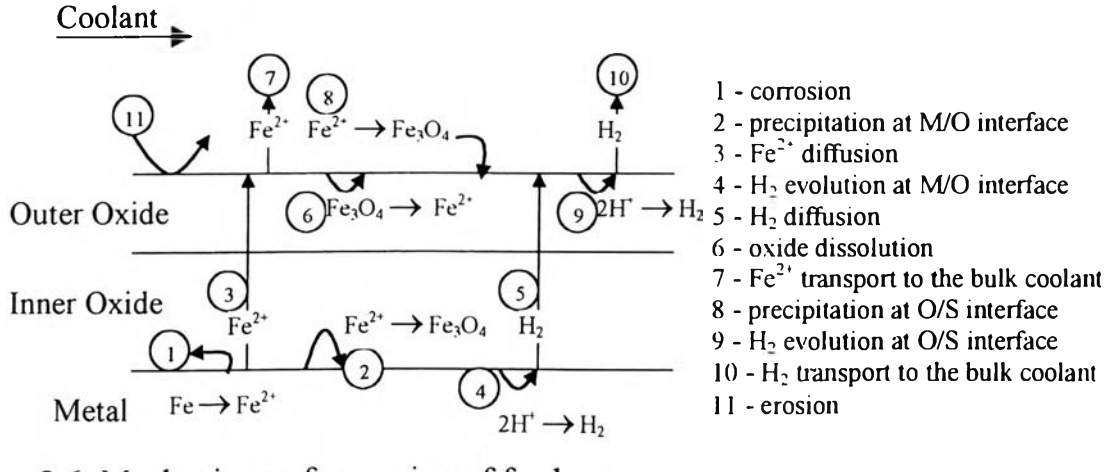

Figure 3.6 Mechanisms of corrosion of feeders.

3.2.1 Corrosion

At the metal surface, there is the corrosion of carbon steel. Iron metal is changed into iron ion form. There is current flowing because of this change. To evaluate the current, it is necessary to develop the electrochemical equations.

$$Fe + H_2O \rightarrow Fe(OH)_2 + 2e^- + 2H^+ \tag{3.3}$$

$$E_{e,1} = 0.14 - 1.98\times10^{-4}T\cdot pH + 4.31\times10^{-5}T\cdot\ln[Fe(OH)_2] \tag{3.4}$$

$$I_{o,1} = nF\frac{k}{h}T\exp\left(-\Delta G^{\neq}_{Fe^{2+}/Fe}/RT\right)C_{Fe(OH)2}\exp\left(-\frac{(1-\beta)nF}{RT}E_{e,1}\right) \tag{3.5}$$

$$I_1 = I_{o,1}\left[\exp\left(\frac{\beta nF}{RT}(E-E_{e,1})\right) - \exp\left(-\frac{(1-\beta)nF}{RT}(E-E_{e,1})\right)\right] \tag{3.6}$$

3.2.2 Precipitation of Dissolved Iron

There is dissolved iron after corrosion takes place. Some of dissolved iron precipitates and forms magnetite at the metal/oxide interface. This oxide replaces the volume of corroded metal. The remained of dissolved iron diffuses through the oxide and forms outer oxide at the oxide/solution interface.

$$Fe(OH)_2 \rightarrow \frac{1}{3}Fe_3O_4 + \frac{2}{3}H^+ + \frac{2}{3}e^- + \frac{2}{3}H_2O \tag{3.7}$$

$$E_{e,2} = -0.75 - 1.98\times10^{-4}T\cdot pH - 1.292\times10^{-4}T\cdot\ln[Fe(OH)_2] \tag{3.8}$$

$$I_{o,2} = nF\frac{k}{h}T\exp\left(-\Delta G^{\neq}_{Fe^{2+}/Fe_3O_4}/RT\right)C_{Fe(OH)2}\exp\left(\frac{\beta nF}{RT}E_{e,2}\right) \tag{3.9}$$

$$I_2 = I_{o,2}\left[\exp\left(\frac{\beta nF}{RT}(E-E_{e,2})\right) - \exp\left(-\frac{(1-\beta)nF}{RT}(E-E_{e\,2})\right)\right] \tag{3.10}$$

At the metal/oxide interface, the volume of oxide replaces the volume of metal loss. Thus,

$$\text{The amount of oxide that forms at this interface} = m\frac{\rho_{ox}}{\rho_{metal}}(1-\phi) \tag{3.11}$$

$$\text{The amount of iron in the oxide} = f' m \frac{\rho_{ox}}{\rho_{metal}} \left(1 - \phi\right) \qquad (3.12)$$

where m = the amount of metal loss per unit area (g/cm^3)

ρ_{ox} = density of oxide (5.2 g/cm^3)

ρ_{metal} = density of metal (7.86 g/cm^3)

ϕ = porosity

f' = mass fraction of iron in oxide (0.723).

Hence,

$$\text{the remainder of dissolved iron} = m - 0.476m\left(1 - \phi\right) \qquad (3.13)$$

3.2.3 Dissolved Iron Diffusion

The dissolved iron that does not form oxide at the metal/oxide interface will diffuse through the pores of the oxide film to the oxide/solution interface.

Fick's law, given

$$J = -D_{eff} \frac{\partial C}{\partial x} \qquad (3.14)$$

$$= D_{eff} \frac{(C_w - C_{os})}{\delta_{eff}} \qquad (3.15)$$

For diffusion through the porous media,

$$D_{eff} = \frac{D\phi}{\tau} \qquad (3.16)$$

In this case, there are two layers of oxide with difference in porosities. The amount of mass flux (J) through each layer is equal.

$$J = \frac{C_w - C_{os}}{\frac{\delta_{eff,i}}{D_{eff,i}} + \frac{\delta_{eff,o}}{D_{eff,o}}} \tag{3.17}$$

$$\delta_{eff} = \frac{\delta}{\rho_{ox}(1-\phi)} \tag{3.18}$$

From Eqs.3.13 and 3.14;

$$0.476\frac{dm}{dt}(1.101+\phi) = \frac{D_{Fe}}{\tau}\frac{1}{\frac{\delta_i}{\rho_{ox}\phi_i(1-\phi_i)} + \frac{\delta_o}{\rho_{ox}\phi_o(1-\phi_o)}}(C_w - C_{os}) \tag{3.19}$$

where J = mass flux (g/cm^2 s)

$\frac{dm}{dt}$ = metal loss rate per area (g/cm^2 s)

D_{eff} = effective diffusivity (cm^2/s)

D_{Fe} = iron diffusivity (cm^2/s)

τ = tortuosity factor

ϕ = porosity

δ_{eff} = effective path length

δ = the amount of oxide in oxide layer per unit area (g/cm^2)

C_w = dissolved iron concentration at wall (cm^3/s)

C_{os} = dissolved iron concentration at oxide/solution interface (cm^3/s).

3.2.4 H_2 Evolution

H_2 evolution takes place at both the metal/oxide interface and the oxide/solution interface.

$$2H^+ + 2e^- \rightarrow H_2 \tag{3.20}$$

$$E_{e.4} = -1.98\times10^{-4}T\cdot pH - 4.31\times10^{-5}T\cdot\ln[H_2] \tag{3.21}$$

$$I_{o,4} = nF\frac{k}{h}T\exp\left(-\Delta G^{\neq}_{H_2/H^+}/RT\right)C_{H_2}\exp\left(-\frac{(1-\beta)nF}{RT}E_{e,4}\right) \quad (3.22)$$

$$I_4 = I_{o,4}\left[\exp\left(\frac{\beta nF}{RT}\left(E-E_{e,4}\right)\right)-\exp\left(-\frac{(1-\beta)nF}{RT}\left(E-E_{e,4}\right)\right)\right] \quad (3.23)$$

At the metal/oxide interface, H_2 evolution can be caused by corrosion and precipitation.

$$\text{The amount of } H_2 \text{ from corrosion } = \frac{MW_{H_2}}{MW_{Fe}}\frac{dm}{dt} = 3.58\times10^{-2}\frac{dm}{dt} \quad (3.24)$$

$$\text{The amount of } H_2 \text{ from precipitation } = \frac{MW_{H_2}}{MW_{oxide}}\frac{\rho_{ox}}{\rho_{Fe}}\frac{dm}{dt}(1-\phi)$$

$$= 5.66\times10^{-3}\frac{dm}{dt}(1-\phi) \quad (3.25)$$

where MW_{H2} = molecular weight of hydrogen (2)

MW_{Fe} = molecular weight of iron (55.85)

MW_{oxide} = molecular weight of oxide (231.55).

$$\text{Total } H_2 \text{ at metal/oxide interface } = 3.58\times10^{-2}\frac{dm}{dt} + 5.66\times10^{-3}\frac{dm}{dt}(1-\phi)$$

$$= 5.66\times10^{-3}\frac{dm}{dt}(7.32-\phi) \quad (3.26)$$

3.2.5 H_2 Diffusion

It is assumed that 90% of the produced H_2 at the metal/oxide interface diffuses through the metal(Tomlinson,1981). Therefore, only 10% of the generated H_2 at this interface diffuses through the oxide layer to the solution.

$$\text{The amount of } H_2 \text{ diffusing through the film } = 0.1\times5.66\times10^{-3}\frac{dm}{dt}(7.32-\varphi)$$

(3.27)

Thus,

$$5.66\times10^{-4}\frac{dm}{dt}(7.32-\phi)=\frac{C_{w_{H_2}}-C_{os_{H_2}}}{\frac{\tau}{D_{H_2}}\left(\frac{\delta_i}{\rho_{ox}\phi_i(1-\phi_i)}+\frac{\delta_o}{\rho_{ox}\phi_o(1-\phi_o)}\right)} \tag{3.28}$$

3.2.6 Mass Transfer of H_2 to Bulk

The amount of H_2 diffusing to oxide/solution interface will transfer to the bulk coolant.

$$h\left(C_{osH_2}-C_{bH_2}\right)=5.66\times10^{-4}\frac{dm}{dt}(7.32-\phi) \tag{3.29}$$

From Eq.3.29,

$$C_{osH_2}=C_{bH_2}+\frac{1}{h}5.66\times10^{-4}\frac{dm}{dt}(7.32-\phi) \tag{3.30}$$

From Eq.3.28 and 3.30,

$$C_{WH_2}=C_{bH_2}+5.66\times10^{-4}\frac{dm}{dt}(7.3d2-\phi)\left(\frac{1}{h}+\frac{\tau}{D_{H_2}}\frac{\delta_i}{\rho_{ox}\phi_i(1-\phi_i)}\right) \tag{3.31}$$

Ferrell and Himmelblau(1967) measured the diffusivity of H_2 at temperatures between 10°C to 55°C. From their work, the diffusivity of H_2 can be obtained by Eq.3.32.

$$D_{H_2}=2.2\times10^{-5}T\exp\left(-\frac{12400}{T}\right) \tag{3.32}$$

where D_{H2} = diffusivity of hydrogen

R = gas constant (8.314 J/mol K)

T = absolute temperature (K).

The mass transfer coefficient (h) for hydrogen in pipe flow can be determined by Eq.3.33.

$$Sh=0.02\,\mathrm{Re}^{0.83}\,Sc^{1/3} \tag{3.33}$$

3.2.7 Oxide Dissolution

When the system is unsaturated as for the outlet feeders, oxide will dissolve into the solution. To calculate the dissolution rate, Eq.3.34 is used.

$$\text{dissolution rate} = k_d F^* (C_{sat} - C_{os}) \tag{3.34}$$

where F^* = surface area factor

C_{sat} = solubility concentration

C_{os} = concentration at oxide/solution interface.

The value of the dissolution rate constant varies with temperature. Using Tremaine and Leblanc(1980) as well as Balakrishnan (1977)'s work, the expression for k_d calculation as a function of temperature is obtained at $pH_{25°C}$ of 10.2.

$$k_d = \exp(-3569/T + 0.0879) \tag{3.35}$$

The solubility of magnetite is the maximum amount of magnetite that can dissolve into the solution. The solubility is a function of temperature and pH. The value of solubility can be obtained by Tremaine and Leblanc's work(1980), Figure 3.7.

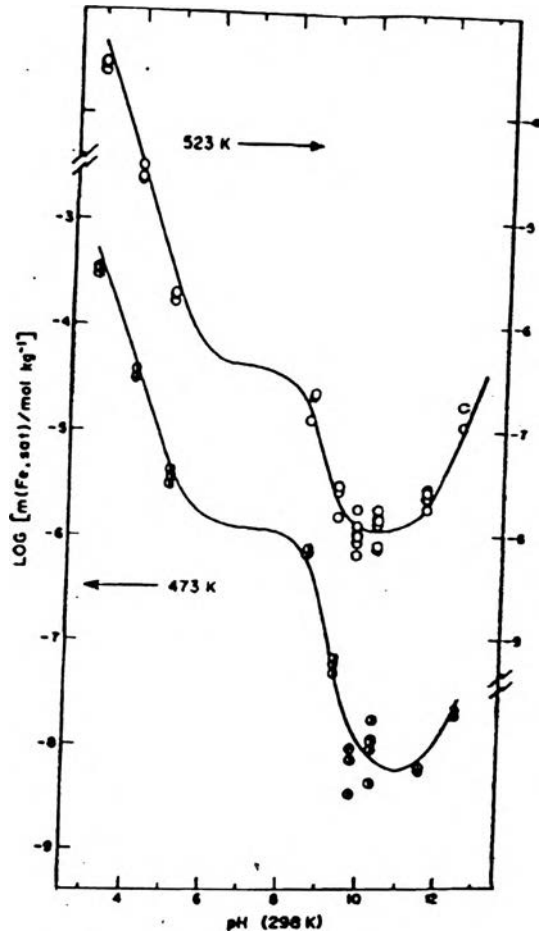

Figure 3.7 Solubilities at 523K and 473K (Tremaine and Leblanc, 1980).

3.2.8 Mass Transfer of Dissolved Iron to Bulk

Dissolved iron at the oxide/solution interface will diffuse to the solution when there is a concentration gradient between the oxide/solution interface and the bulk solution.

rate of dissolved iron transport to bulk $= h(C_{os} - C_b)$ (3.36)

where h = mass transfer coefficient.

the correlation for the mass transfer coefficient for pipe flow with a diffusivity of 4.1×10^{-4} cm^2/s is evaluated by Eq.3.37.

$$h = 6.37 \times 10^{-4} \frac{U^{0.82}}{d^{0.18}} \tag{3.37}$$

where U = velocity (m/s)

d = diameter of pipe (m).

Iron at the oxide/solution interface is transferred to the bulk solution. This results in a bulk concentration change along the feeders.

The balance for iron in a cylindrical pipe shell;

$$\pi \frac{d^2}{4} \Delta x \frac{\partial C_b}{\partial t} = \left(\pi C_b \frac{d^2}{4} U \Big|_x - \pi C_b \frac{d^2}{4} U \Big|_{x+\Delta x} \right) + \pi d \Delta x h (C_{os} - C_b) \tag{3.38}$$

Dividing Eq.3.38 by $\pi \frac{d^2}{4} \Delta x$;

$$\frac{\partial C_b}{\partial t} = U \frac{\partial C_b}{\partial x} - \frac{4h}{d} (C_{os} - C_b) \tag{3.39}$$

3.2.9 Erosion

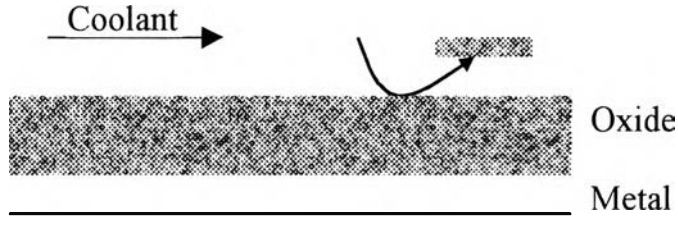

Figure 3.8 Erosion of oxide.

The erosion of outlet feeders is caused by the velocity of coolant. The high velocity affects high wall shear stress in the feeders. Therefore, time for the spalling of particles from the oxide is small. The oxide thickness is lower when the velocity is higher. The time for erosion events depends not only on velocity or shear stress but also on the size of the particle

and the porosity as well as dissolution. The correlation of this time is expressed in Eq.3.40.

$$t = \frac{sd}{v^2 \phi k_d \Delta C} \tag{3.40}$$

where s = proportionality spalling (erosion) constant

d = diameter of particle to be removed (μm)

v = velocity (cm/s)

ϕ = porosity

k_d = dissolution rate constant (cm/s)

ΔC = concentration difference between solubility and concentration at surface (g/cm^3).

In the saturated system as from inlet feeders, there is no dissolution. Thus, the Eq.3.40 is rewritten for saturated system as,

$$t = \frac{sd}{v^2 \phi} \tag{3.41}$$

For the size of spalled particle, Lang (2000) proposed a reciprocal distribution of particle size. A small particle is removed from the oxide layer more often than a large particle.

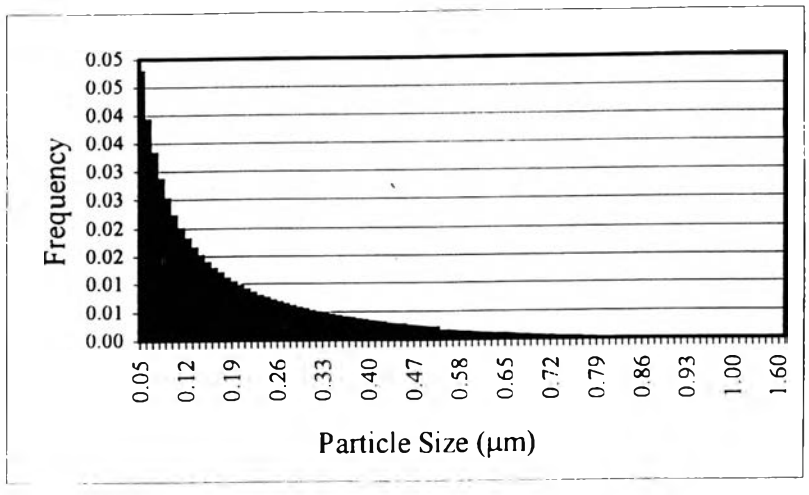

Figure 3.9 Size distribution(Lang, 2000).

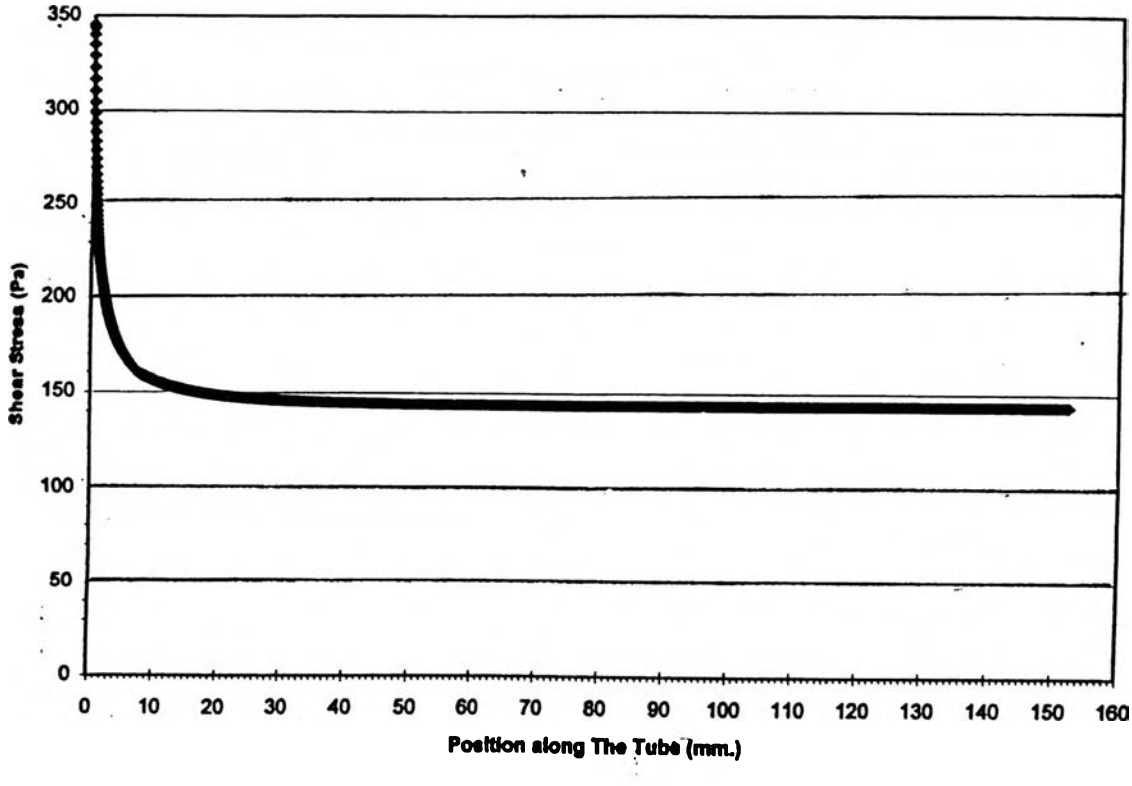

Figure 3.10 Shear stress for tube probe with fluid velocity of 10m/s, from FLUENT (Supa-Amornkul, 2001).

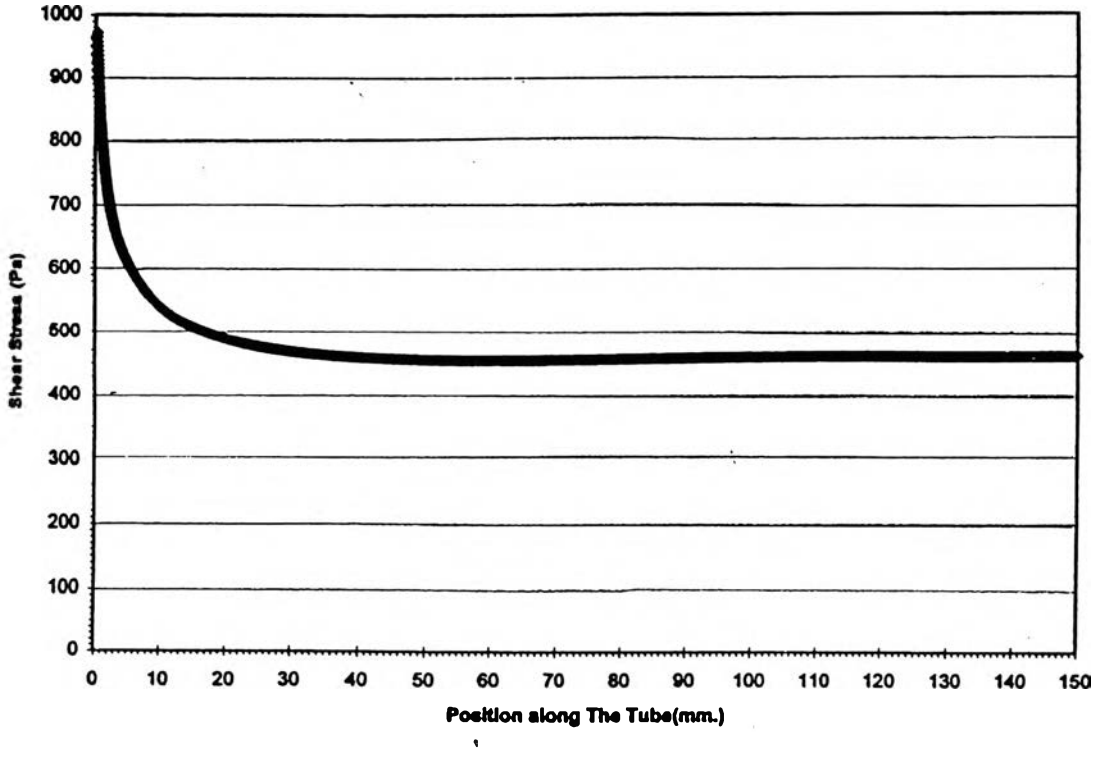

Figure 3.11 Shear stress for tube probe with fluid velocity of 20m/s, from FLUENT (Supa-Amornkul, 2001).

The time for erosion event is also affected by the velocity that causes the shear stress in the feeders. FLUENT, the Computational Fluid Dynamics (CFD) code, is used to determine wall shear stress along outlet feeders and probes in the test loop.

Figures 3.10 and 3.11 are the shear stress distribution along the tube probe at fluid velocities of 10m/s and 20m/s, respectively. These distributions were computed by using FLUENT code (Supa-amornkul, 2001). It is indicated that the high wall shear stress takes place at the entrance for both tubes, due to the high velocity gradients in this region. The higher wall shear stress in Figure 3.11 than in Figure 3.10 indicates that higher velocity yields in higher shear stress. From the difference in wall shear stress at different areas

the shear stress enhancement is added in the denominator of Eqs.3.40 and 3.41. This enhancement is the ratio of the local shear stress to the shear stress at fully developed flow.

3.2.10 Overall Equations

The oxide layer will protect the metal surface from corrosion, therefore, a thick oxide layer reduces the corrosion rate of the metal.

The inner oxide thickness is obtained by an iron balance on the inner layer.

Oxide growth = precipitation – dissolution – removal term (3.42)

$$0.723\frac{d\delta_i}{dt} = 0.476\frac{dm}{dt}(1-\phi) - \lambda_i k_d F^*(C_{sat} - C_{os}) - B\rho_{H_2O}U^2 \quad (3.43)$$

where δ_i = the amount of oxide in inner per unit area

λ_i = 1 when $C_{sat} > C_{os}$ and $\delta_i \neq 0$

= 0 otherwise

B = removal constant ((g_{Fe}/g_{H2O}) s/cm)

U = velocity (cm/s).

For the outer oxide layer thickness;

Oxide growth = –dissolution – removal term (3.44)

$$0.723\frac{d\delta_o}{dt} = -\lambda_o k_d F^*(C_{sat} - C_{os}) - B\rho_{H_2O}U^2 \quad (3.45)$$

where δ_o = the amount of oxide in outer per unit area

λ_o = 0 when $C_{sat} > C_{os}$ and $\delta_o = 0$

= 1 otherwise

Concentration at the oxide/solution interface can be determined from Eq.3.28;

$$C_{os} = C_w - 0.476\frac{dm}{dt}(1.101+\phi)\frac{\tau}{D_{Fe}}\left[\frac{\delta_i}{\rho_{ox}\phi_i(1-\phi_i)}+\frac{\delta_o}{\rho_{ox}\phi_o(1-\phi_o)}\right] \quad (3.46)$$

At the oxide/solution interface, the iron balance is as Eq.3.47;

diffusion + dissolution = mass transfer (3.47)

$$0.476\frac{dm}{dt}(1.101+\phi)+k_dF^*(C_{sat}-C_{os})=h(C_{os}-C_b) \quad (3.48)$$

From Eq.3.48;

$$C_{os} = \frac{1}{h+k_dF^*}\left(0.476\frac{dm}{dt}(1.101+\phi)+k_dF^*C_{sat}+hC_b\right) \quad (3.49)$$

Eq.3.49 can be used to calculate C_{os}, the same as Eq.3.46. Let Eq.3.46 equal Eq.3.49, then the corrosion rate expression is obtained as

$$\frac{dm}{dt} = \frac{C_w - \frac{1}{\left(h+k_dF^*\right)}\left(k_dF^*C_{sat}+hC_b\right)}{0.476\left(1.101+\phi\right)\left[\frac{\tau}{D_{Fe}}\left(\frac{\delta_i}{\rho_{ox}\phi_i\left(1-\phi_i\right)}+\frac{\delta_o}{\rho_{ox}\phi_o\left(1-\phi_o\right)}\right)+\frac{1}{h+k_dF^*}\right]} \quad (3.50)$$

Since the model mentioned above is complicated with electrochemical calculation. There are many ideas about electrochemical effect. The new model that based on reaction and mass transfer was proposed (Steward, 2000). This new model did not concern with electrochemical calculation. It is described in appendix E.

3.3 Computation

The primary coolant loop is divided into segments. The boundary of each segment is called a node. For the outlet feeder, there are seven nodes for

the entrance section, the first bend, down stream of the first bend, and four nodes along the straight pipe, Figure 3.12.

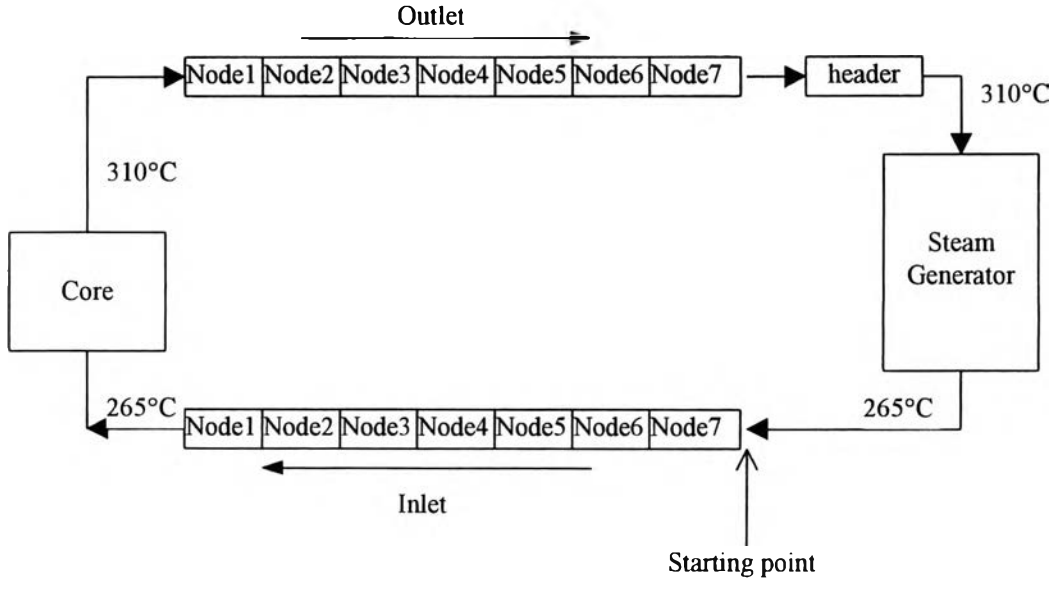

Figure 3.12 Computational segments in the loop.

The probe in the test loop, can be divided into two nodes for the outlet and none for the inlet. This is due to the length probe and the less complicated geometry.

In this computation, the time dependence of the bulk concentration can be neglected because the coolant flows around the loop in a short period of time. Furthermore, the corrosion of carbon steel is not sensitive to time increments of seconds, except in the initial stage when the corrosion rate is very high. The data input for feeders and variables are attached in appendix A. Visual Basics in Microsoft Excels program is used for computation. The program code is in appendix B. The program for the probe is attached in appendix C.